In vivo molecular mediators of cancer growth suppression and apoptosis by selenium in mammary and prostate models: lack of involvement of *gadd* genes

Weiqin Jiang,[2,3] Cheng Jiang,[1,2] Hongying Pei,[2] Lei Wang,[1] Jinhui Zhang,[1] Hongbo Hu,[1] and Junxuan Lü[1,2]

[1]Hormel Institute, University of Minnesota, Austin, Minnesota; [2]AMC Cancer Research Center, Denver, Colorado; and [3]Cancer Prevention Laboratory, Colorado State University, Fort Collins, Colorado

Abstract

We used acute selenium (Se) treatments (i.e., daily single oral gavage of 2 mg Se per kilogram of body weight for 3 days) of female Sprague-Dawley rats bearing 1-methyl-1-nitrosourea–induced mammary carcinomas to increase the probability of detecting *in vivo* apoptosis and the associated gene/protein changes in the cancerous epithelial cells. The results show that whereas control carcinomas doubled in volume in 3 days, Se-methylselenocysteine and selenite treatments regressed approximately half of the carcinomas, accompanied by a 3- to 4-fold increase of morphologically observable apoptosis and ~40% inhibition of 5-bromo-2′-deoxyuridine index of the cancerous epithelial cells. The mRNA levels of *growth arrest-DNA damage inducible 34* (*gadd34*), *gadd45*, and *gadd153* genes were, contrary to expectation, not higher in the Se-treated carcinomas than in the gavage or diet restriction control groups. The gadd34 and gadd153 proteins were localized in the nonepithelial cells and not induced in the cancer epithelial cells of the Se-treated carcinomas. On the other hand, both Se forms decreased the expression of cyclin D1 and increased levels of P27Kip1 and c-Jun NH_2-terminal kinase activation in a majority of the mammary carcinomas. Furthermore, the lack of induction of *gadd* genes *in vivo* by methylseleninic acid was confirmed in a human prostate xenograft model in athymic nude mice. In summary, these experiments showed the induction of cancer epithelial cell apoptosis and inhibition of cell proliferation by Se *in vivo* through the potential involvement of cyclin D1, P27Kip1, and c-Jun NH_2-terminal kinase pathways. They cast doubt on the three *gadd* genes as mediators of Se action *in vivo*. [Mol Cancer Ther 2009;8(3):682–91]

Received 9/22/08; revised 11/18/08; accepted 12/8/08; published OnlineFirst 3/10/09.

Grant support: American Institute for Cancer Research grant 97A083 and National Cancer Institute grants CA95642 and CA126880.

The costs of publication of this article were defrayed in part by the payment of page charges. This article must therefore be hereby marked *advertisement* in accordance with 18 U.S.C. Section 1734 solely to indicate this fact.

Note: The study with rat mammary cancer model was accomplished while W. Jiang, H. Pei, C. Jiang, and J. Lü were on the staff of the AMC Cancer Research Center, Denver, CO 80214. An abstract describing this work was presented at the 1998 AACR Annual Meeting. W. Jiang, et al. Differential effects of chemopreventive selenium compounds on mammary cancer cell proliferation and cell death *in vivo*.

Requests for reprints: Junxuan Lü, Hormel Institute, University of Minnesota, 801 16th Avenue NE, Austin, MN 55912. Phone: 507-437-9680; Fax: 507-437-9606. E-mail: jlu@hi.umn.edu

doi:10.1158/1535-7163.MCT-08-0908

Introduction

Selective induction of neoplastic cell apoptosis may be a potential mechanism to mediate the anticancer activity of selenium (Se). *In vivo*, it has been shown that Se-enriched garlic, of which Se-methylselenocysteine (MSeC) constitutes a major Se component, exerts a lasting protective effect when provided for 1 month immediately after 1-methyl-1-nitrosourea (MNU) exposure as great as when provided throughout the duration of the chemoprevention study (1, 2). This finding indicates that the chemopreventive intake of Se may exert such permanent protection against cancer development by inducing the deletion of transformed mammary epithelial cells *in vivo* through apoptosis.

We and others have investigated the proapoptotic effects of Se on mammary and prostate cancer cells and leukemia cells *in vitro* (3–7) and have identified distinct pathways of signaling and execution with respect to different Se metabolite pools (8). The objectives of the current work were to investigate the *in vivo* proapoptotic and therapeutic effects of Se in preclinical animal models and to characterize the expression changes of selected genes as potential *in vivo* molecular targets/biomarkers of the anticancer action.

Regarding the choice of potential molecular targets for investigation, we have, in earlier work with cell culture models, documented a differential induction of three *growth arrest and DNA damage inducible* (*gadd*) genes in mammary cancer epithelial cells by Se compounds that entered two different metabolite pools: selenite (SEL) as a precursor for the genotoxic hydrogen selenide pool and MSeC and methylselenocyanate as precursors to the nongenotoxic methylselenol pool (5, 9). The *gadd* genes were initially identified by their inducibility after Chinese hamster ovary cells were exposed to the genotoxic agent methyl methanesulfonate (10). These genes are often, but not always, coordinately induced upon exposure of mammalian cells to genotoxic stress or growth arrest conditions (11–13). *gadd34* is a homologue of the murine myeloid differentiation gene *MyD116* (14). *gadd45* is homologous to but distinct from the murine *MyD118* (14)

and has been found to interact with proliferating cell nuclear antigen to mediate DNA repair activity and is a transcriptional target of p53 (15). The *gadd153* product is a homologue of murine CHOP-10, a member of the CAAT/enhancer binding protein family of transcription factors (13). It is highly inducible by DNA cross-links and by nutrient deprivation (12) and has been linked to endoplasmic reticulum stress responses (16). The growth arrest and prodifferentiation properties of the *gadd* gene products and our observation of their induction by Se exposure of mammary cancer epithelial cells in cell culture models (5, 9) prompted our initial effort, more than a decade ago, to link the *in vitro* biochemical changes with *in vivo* proapoptotic action. Recent studies with PC-3 prostate cancer cells have confirmed the induction of *gadd153 in vitro* by methylseleninic acid (MSeA), another putative methylselenol precursor compound (7, 17, 18). However, whether the *gadd* genes play a mediator role *in vivo* for the anticancer effects of Se has not been evaluated.

Tumor size is largely a function of the balance between cell proliferation rate and cell death rate. Aberrant mitogenic and survival signaling pathways are often associated with neoplasia and interfering with such signaling can lead to cell cycle arrest and apoptosis. Although the MAPK1/2/ERK1/2 pathway has been primarily involved with proliferation and survival, the stress-activated protein kinases/c-Jun NH_2-terminal kinases (JNK) have recently been linked to cellular apoptosis response to stress factors, including DNA damage, genotoxic agents, UV and ionizing radiation, cold and heat shock, osmotic pressure, genotoxicity, cytokines, or growth factor withdrawal in several cell lines (19). The balance of MAPK1/2 and JNK seems to be a critical determinant of neuronal cell survival (20) and other cell types (21). Cyclins and cyclin-dependent kinases and their regulatory partners, such as P27Kip1 and P21Cip1, are crucial for controlling cell cycle entry and progression (22, 23). Cyclin D1 seems to be particularly critical for mammary epithelial proliferation because in adult D1 knockout mice, the mammary epithelial compartment fails to undergo the massive proliferative changes associated with pregnancy despite normal levels of ovarian steroid hormones (24).

We therefore examined the expression of the three *gadd* genes; the phosphorylation status of ERK and c-Jun (JNK substrate); and the expression of cyclin D1, P21Cip1, and P27Kip1 in Se-exposed mammary carcinomas to explore their potential as *in vivo* targets of Se regulation of apoptosis and cell proliferation. In addition, we sought to extend and cross-validate the findings from the mammary carcinoma model into a human prostate cancer xenograft model in athymic nude mice.

Materials and Methods

Chemicals and Reagents

Sodium selenite pentahydrate was purchased from J.T. Baker, Inc. MSeC used for mammary cancer study was kindly provided by Dr. Howard Ganther (University of Wisconsin, Madison, WI). MSeC used for the xenograft study was purchased from LKT Labs. Methaneseleninic acid (same as MSeA, >95%, white powder) was purchased from Sigma Chemical Company. Antibodies to gadd proteins, β-actin, and Bcl-2 were purchased from Santa Cruz Biotechnology. The phosphospecific antibodies to pERK1/2 and p-Ser63-JUN were purchased from New England Biolabs. P27kip1 and cyclin D1 antibodies were purchased from NeoMarker, Inc. The anti–5-bromo-2′-deoxyuridine (BrdUrd) antibody was purchased from Becton Dickinson.

Rat Mammary Carcinogenesis Model

This experiment was reviewed and approved by the Institutional Animal Care and Use Committee of AMC Cancer Research Center, Denver, Colorado, and was carried out by H.P. and J.L. Female Sprague-Dawley rats were purchased from Taconic Farms at 20 d of age. Rats were fed a modified AIN-93 diet. Rats were housed three per cage in an environment-controlled animal room in the AMC Animal Facility maintained at 22 ± 1°C with 50% relative humidity and a 12-h light/12-h dark cycle. At 21 d of age, animals were each given an i.p. injection of 50 mg MNU [dissolved in acetic acid–acidified saline (pH 4) at a concentration of 14 mg/mL] per kilogram of body weight for the induction of mammary carcinogenesis (25). Starting 4 wk post–carcinogen administration, all rats were palpated thrice per week for the detection of mammary tumors. Tumor dimensions were measured using a Vernier caliper. In this model, palpable tumor growth was very rapid, doubling in volume every 3 d. The majority of the tumors in this short-term model were estrogen responsive as in the standard model (26).

Selenium Treatment and Other Experimental Manipulations

When the largest mammary tumor in a tumor-bearing rat attained or exceeded ~1 cm on the longest dimension, the tumor-bearing rat was randomly assigned to one of five treatment groups (n = 4-6 rats): (*a*) water oral gavage control using a 1-mL plastic tip delivered through a Pipetman to the back of the tongue, (*b*) once per day oral gavage of 2 mg Se as MSeC per kilogram of body weight, (*c*) once per day gavage of 2 mg Se as sodium selenite per kilogram of body weight, (*d*) diet restriction (to 70% *ad libitum* intake), and (*e*) bilateral ovariectomy. The Se treatment was repeated daily for a total exposure of 6 mg of Se per kilogram of body weight over the 3-d duration. The Se dose chosen was ~5 to 10 times of the daily Se intake in a typical chemoprevention setting. Tumor samples were harvested 24 h after the third Se dose.

We included ovariectomy and diet restriction groups for comparison with the following rationale. The majority of MNU-induced mammary carcinomas are dependent on and sensitive to ovarian hormones (26). Therefore, ovariectomy was used as a positive control for apoptosis and growth inhibition of cancerous mammary epithelial cells to compare and contrast similarities and distinctions in the apoptosis and growth-regulatory mechanisms induced by

Se and ovarian oblation. Because intake of Se in much excess of its nutritional requirement can lead to adverse effects on food intake and body weight, diet restriction was used to control for nonspecific effects associated with body weight loss.

Tumor Size and Necropsy

The size of a tumor was measured as its two largest perpendicular dimensions and these data were used to compute volume using the formula for an ellipsoid. Tumor-bearing rats were killed 24 h after the third Se dose. A BrdUrd pulse-labeling technique was used to assess the proliferation rate of the cancerous epithelial cells (27). Rats were given an i.p. injection of 50 mg BrdUrd (dissolved in saline; Sigma Chemical Co.) per kilogram of body weight 3 h before euthanasia. All tumors (including those for which size measures were not taken) were excised and cut in the middle. Two slices were fixed in neutral buffered formalin and methacarn (acidic alcohol fixative), respectively. The rest of the tumor tissue was frozen in liquid nitrogen for assessment of biochemical and gene expression changes. Because of the heavy demand of tissues for the various assays, it was necessary to do some assays on different sets of tumors and, therefore, not all measured variables could be correlated.

Human DU145 Prostate Cancer Xenograft Model in Athymic Nude Mice

The animal use protocol was approved by the Institutional Animal Care and Use Committee of the University of Minnesota and carried out at the Hormel Institute's animal facility. Male BALB/c athymic nude mice were purchased from NxGen BioSciences at 4 to 5 wk of age. They were housed in a specific pathogen–free room with free access to water and commercial rodent chow. Animals are maintained in clean HEPA-filter top covered cages. Cages, bedding, cage tops, and water bottles were washed and maintained separately from other animal materials and supplies. After 2 wk of quarantine, each mouse was inoculated by s.c. injection with DU145 cells and tumor measurements and selenium treatments have been described recently (28).

To assess the early dynamic processes of apoptosis signaling in the target human prostate cancer cells *in vivo*, we treated tumor-bearing mice with MSeA at 4 mg per kilogram of body weight for 24 and 72 h when the xenograft has grown to ~150 mm^3 (3 wk after inoculation). Tumors from five to six mice of each group were pooled (approximately equal weight) for preparation of tissue lysate for Western blot analysis of biomarkers related to caspase-mediated apoptosis and gadd protein abundance.

Apoptotic Indices

For the rat mammary cancer model, apoptosis of the cancerous mammary epithelial cells was morphologically determined on H&E-stained sections of the formalin-fixed portion of the carcinomas. The primary criteria for the identification of apoptotic cells were cell shrinkage, nuclear condensation, fragmentation, apoptotic bodies, and lack of inflammatory components (29). The apoptotic index (i.e., the percentage of apoptotic cells over total cells counted) was determined on 20 ×200 fields of cancerous epithelial cells, excluding regions of gross necrosis. For the xenograft tumors, apoptosis was detected by terminal deoxyribonucleotide transferase–mediated nick-end labeling (TUNEL) assay according to the manufacturer's instructions (28).

BrdUrd Index for Cell Proliferation Estimation

Methacarn-fixed mammary carcinomas were thin sectioned (5 mm) and stained for BrdUrd immunohistochemically by a method described by McGinley et al. (27). An anti-BrdUrd antibody (1:40) was used to detect nuclei that have incorporated BrdUrd into their DNA. After a light nuclear counterstain with hematoxylin, the BrdUrd-labeled and unlabeled nuclei were counted at ×400 with a computer-assisted image analyzer using the Quantitative Nuclear Antigen Program Version 3.0 (CAS-200, Becton Dickinson/Cellular Analysis Systems) as described elsewhere (30). The proliferation index (i.e., the percentage of labeled cells over total cells counted) was determined by counting 20 fields of cancerous epithelial cells per slide (~2,000 cells), excluding gross necrotic regions.

Steady-State mRNA Level by Reverse Transcription-PCR

Total RNA was extracted from the frozen carcinoma tissues using the RNAzol B reagent (Tel-Test, Inc.). Total RNA (0.5 μg) was reverse transcribed using anchored oligo$(dT)_{10}$ as the primers. The PCR primers were synthesized commercially (Integrated DNA Technologies, Inc.). The sequences of primers and PCR setting information were described earlier (9).

For real-time reverse transcription-PCR (RT-PCR), total RNA were extracted using RNeasy kit (Qiagen). One microgram of total RNA was used for cDNA synthesis with oligo-dT primer and SuperScript II Reverse Transcriptase (Invitrogen) in a 20-μL reaction system and 5 μL of diluted cDNA (1:20) were used in each 25-μL real-time PCR reaction using the Fast Start Universal SYBR Master with ROX (Roche) with an ABI 7500 Real-Time PCR System (Applied Biosystems). A standard curve was generated in each assay and used to derive the copy number of each transcript. β-Actin was selected as an internal standard and all the raw data were expressed as the ratio of the copy number of selected gene to β-actin. Statistical significance was determined by an unpaired, two-tailed Student's *t* test.

Western Blot Analyses

The expression levels of growth regulatory– and cell death–associated proteins were assessed by Western immunoblot analyses of mammary carcinoma extracts using enhanced chemiluminescence detection (31). The total protein content of extracts was determined by the Bradford dye binding assay (Bio-Rad Laboratories). After probing for the protein of interest, the membranes were stripped and reprobed for β-actin to control for gel loading differences and protein integrity. The X-ray films were digitized using a transmission scanner and the signal intensity was quantitated using the UN-SCAN-IT gel scanner software (Silk Scientific, Inc.). The signals (pixels) for the proteins were normalized to that of the corresponding β-actin. The normalized expression data were used for statistical evaluations.

Immunohistochemical Localization of Proteins

Formalin-fixed and paraffin-embedded mammary carcinomas were thin sectioned (5 mm) and immunohistochemically stained for gadd34, gadd153, and P27Kip1 proteins. Antigen retrieval was done on these sections in 10 mmol/L sodium citrate buffer (pH 6.0) by microwave heating.

Statistical Analyses

Unless otherwise stated, data are reported as mean ± SE. ANOVA and/or rank-order tests, when the variance was not normally distributed, were carried out with the Systat package (Systat, Inc.).

Results

Response of Established Rat Mammary Carcinomas to Acute Se Exposure

Daily single oral gavage treatment (delivered to the back of tongue) of mammary tumor-bearing rats with either MSeC or SEL for 3 days resulted in a 6% or 3% body weight loss in comparison with pretreatment weight, respectively, whereas the control rats increased body weight at the same time by 5% (Fig. 1A). These treatments elevated the liver Se content 4.6-fold and 3.3-fold, respectively (Fig. 1B). Because sustained caloric restriction and associated body weight loss have been shown to inhibit mammary carcinogenesis in this model (32), we therefore instituted a dietary restriction control to investigate the proapoptotic activity of Se exposure that was independent of body weight loss.

The tumor volume of the gavage control rats increased in 3 days by 125 + 48% (mean ± SE; Fig. 1C). The vast majority of the tumors in either MSeC- or SEL-treated tumor-bearing rats did not grow in the same duration. In fact, four of eight MSeC-treated tumors and four of seven SEL-treated tumors showed regression, respectively, relative to pretreatment volumes. The magnitude of Se-induced tumor size changes was almost as much as that induced by bilateral ovariectomy, a positive control for apoptosis induced by estrogen deprivation (Fig. 1C). On the other hand, diet restriction that resulted in a comparable degree of body weight loss (i.e., 6% of pretreatment weight) did not inhibit tumor growth with a tumor volume increase in 3 days of 105 ± 18% (Fig. 1C). Taken together, the tumor volume

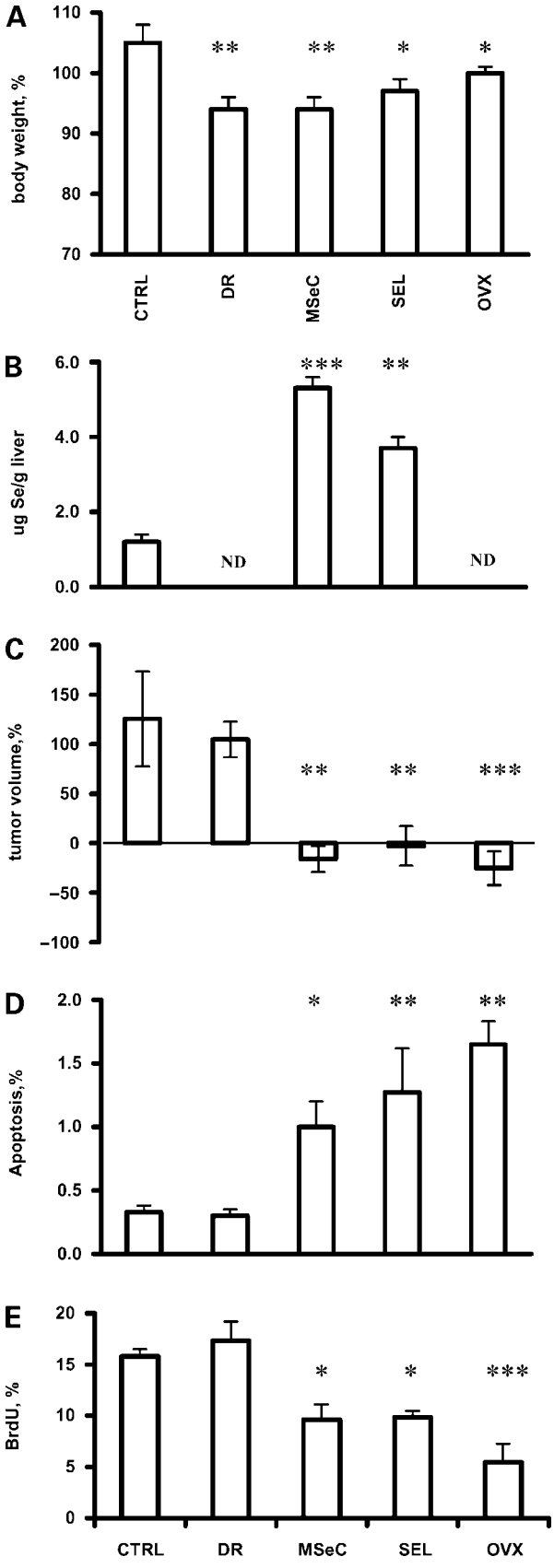

Figure 1. Effects of daily single gavage of Se compounds, dietary restriction, or ovariectomy in tumor-bearing rats on body weight (**A**), liver Se content (**B**), carcinoma volume (**C**), the rate of mammary tumor epithelial cell apoptosis (**D**), and the rate of mammary tumor epithelial cell proliferation (**E**), assessed at 3 d after the initiation of each experimental manipulations. *CTRL,* gavage control group; *MSeC,* methylselenocysteine-treated group, 2 mg Se/kg body weight per day; *SEL,* selenite-treated group, 2 mg Se/kg body weight per day. **A,** body weight relative to day 0 (n = 4–6 rats). **B,** liver Se content on wet tissue basis. *ND,* not determined for the dietary restriction and ovariectomy groups (n = 4–6). **C,** tumor volume change in reference to pretreatment value on day 0 (n = 5–8). **D,** incidence of morphologically identifiable apoptotic cells in cancerous mammary epithelial cells, excluding gross necrotic areas. **E,** percentage of cancerous mammary epithelial cells incorporating BrdUrd, excluding gross necrotic areas. *Columns,* mean; *bars,* SE. Statistical difference from gavage control: *, $P < 0.05$; **, $P < 0.01$; ***, $P < 0.001$.

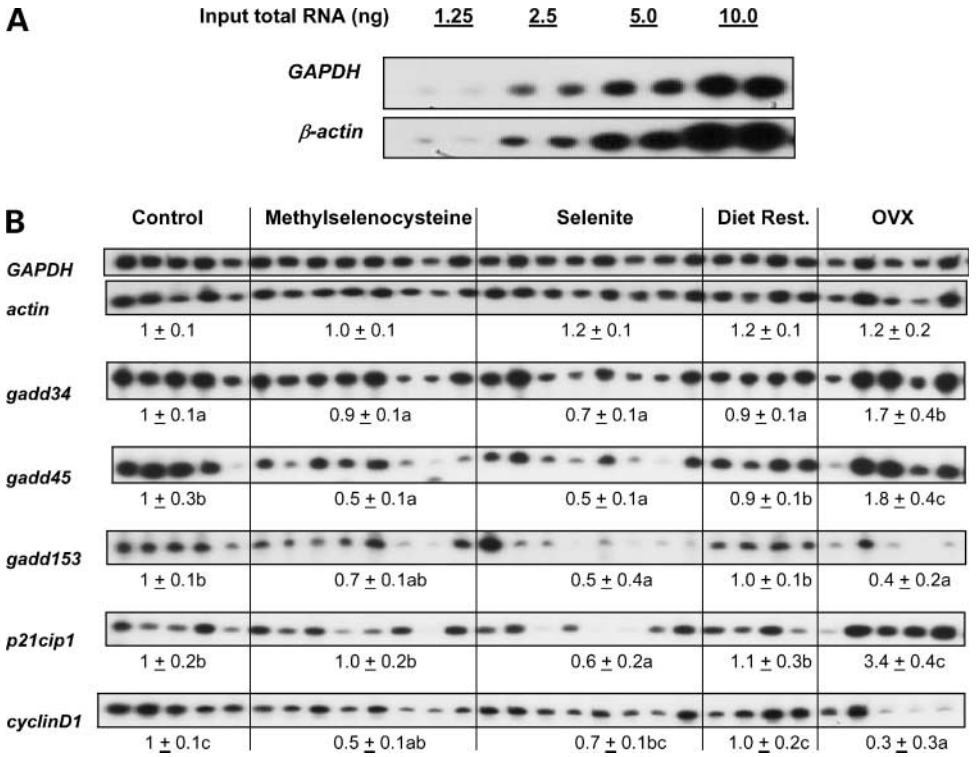

Figure 2. RT-PCR analyses of the steady-state mRNA level in mammary carcinomas. **A,** serial dilution of a mammary tumor cDNA sample to show linearity of detection of two housekeeping genes, *gapdh* and *actin*. **B,** RT-PCR analyses of the steady-state mRNA level of *gadd, p21*, and *cyclin D1* genes in mammary carcinomas after acute treatments with selenium compounds or ovariectomy. The PCR primers and conditions were as published (9). An equivalent of 20 ng of total RNA was used for each sample. Each lane is an individual carcinoma. The housekeeping genes *gapdh* and *actin* were evaluated as normalization controls for loading differences. The normalized pixel intensity values are mean ± SE. Data were analyzed by ANOVA with post hoc ranking. Means among groups in a same row with different superscripts were significantly different ($P < 0.05$).

data (Fig. 1C) indicated that the vast majority of established mammary tumors were responsive to the acute delivery of Se compounds and such a response could not be accounted for by the associated body weight loss.

Mammary Tumor Epithelial Cell Apoptosis *In vivo*

As a positive control of mammary tumor epithelial apoptosis, ovariectomy led to a 5-fold increase in the incidence of morphologically observable epithelial apoptosis when examined 3 days after surgery (Fig. 1D). Tumors in MSeC-treated and SEL-treated rats showed a 3-fold and 4-fold increase in apoptosis, respectively. Dietary restriction of the tumor-bearing rats did not increase the incidence of apoptosis of the mammary tumor epithelial cells.

Mammary Tumor Epithelial Cell Proliferation *In vivo*

As would be expected of the inhibitory effect of estrogen depletion on mammary epithelial proliferation, the rate of cell proliferation measured as BrdUrd incorporation in the mammary tumors was decreased by 65% by ovariectomy (Fig. 1E). The epithelial BrdUrd index of mammary tumors that showed regression after MSeC or SEL exposure was decreased by 40% in comparison with the gavage control tumors (Fig. 1E). Dietary restriction did not decrease the BrdUrd index of the mammary tumor epithelial cells, indicating that the weight loss associated with Se exposure could not account for the decreased BrdUrd incorporation.

Steady-State Transcript (mRNA) Level of *gadd* and Selected Growth Regulatory Genes

The mRNA level in individual mammary tumors from the various groups was detected by RT-PCR (Fig. 2). We tested the linearity of RT-PCR detection of increasing amount of input RNA as shown for the two housekeeping genes, *gapdh* and *β-actin* (Fig. 2A). For the tumor samples, the expression level of *β-actin*, when normalized to *gapdh* used as an internal control, was essentially constant across all groups (Fig. 2B). Diet restriction did not affect the mRNA level of all the genes examined. Contrary to the induction effects reported for cell culture (5, 9), exposure of tumor-bearing rats to either form of Se did not increase the mRNA level of the three *gadd* genes in the mammary tumors that underwent significant growth inhibition and even regression (Fig. 2B). In fact, the expression level of *gadd45* and *gadd153* in a significant proportion of the Se-treated tumors was lower than the gavage or diet restriction controls (Fig. 2B). The mRNA level of P21Cip1 was not increased by Se treatments and was even lower in some of the SEL-treated carcinomas. The mRNA level of cyclin D1 was decreased by 50% and 30% by MSeC and SEL treatment, respectively (Fig. 2B). The Se treatment effects on cyclin D1 and *gadd153* expression were in similar trend as those of ovariectomy. However, ovariectomy led to modest increases of the expression of *gadd34* and *gadd45* and much greater induction of *P21Cip1*, in contrast to the Se treatments, which decreased the mRNA abundance of these genes.

In situ Localization of Gadd Proteins and P27Kip1

Because RT-PCR was done on mammary tumor tissues with no ability to distinguish the cell type origin (cancer epithelial versus stromal and other cell types) of the gene/protein expression changes, we performed immunohistochemistry to determine the expression patterns of gadd34

and gadd153 proteins in the rat mammary tumors. Gadd34 protein was localized to the nonepithelial stromal components, especially in endothelial cells lining tumor microvessels (Fig. 3). Gadd34 protein expression was not detected in mammary tumor epithelial cells of tumor-bearing rats exposed to either MSeC or SEL (Fig. 3; note the absence of staining in glandular epithelial cells). Gadd153 staining had an even more restrictive pattern than that of gadd34, localizing almost exclusively to microvessels (not shown). Se treatment of the tumor-bearing rats did not increase the expression of gadd153 protein in the tumor epithelial cells. The nonepithelial expression patterns along with the lack of induction at the mRNA level did not support an association of the *gadd* expression with the observed *in vivo* antiproliferative and proapoptotic effects of Se on mammary tumor epithelial cells.

The P27kip1 staining in the gavage control carcinomas was weak in the epithelial cells (Fig. 3), whereas uninvolved mammary ducts contained strong epithelial staining (not shown). SEL and ovariectomy significantly increased the expression of P27 protein in the mammary cancer epithelial cells; however, the effect of MSeC on P27 staining was less dramatic than that of SEL: The relative P27 staining intensity (by CAS image analyses) in the cancerous epithelial cells in comparison with the control group (1 ± 0.1, mean $\pm$ SE, $n = 4$) were 1.8 ± 0.5 ($n = 5$), 5.6 ± 1.2 ($n = 7$), and 4.6 ± 1.5 ($n = 4$) for MSeC, SEL, and ovariectomy groups, respectively (Fig. 3). P21Cip1 staining was nuclear and localized predominantly in mammary epithelial cells (not shown). In contrast to the more uniform staining of P27 in epithelial cells, P21 staining was sporadically distributed among cancer epithelial cells and the proportion of cells staining positive for P21 was not increased by Se treatment.

Expression Changes of Selected Growth- and Apoptosis-Regulatory Proteins

We next examined the expression level of cell proliferation–related cyclin D1 and ERK activation status (by phosphorylation) and the apoptotic regulatory Bcl-2 expression and JNK activation by Western blot analyses (Fig. 4). The cyclin D1 protein level was decreased in most tumors in the Se-treated rats and in ovariectomized rats (Fig. 4), in agreement with mRNA expression patterns (Fig. 2B). The levels of phosphorylated ERK (pERK1/2) were not significantly decreased in tumors treated with either Se or by ovariectomy (Fig. 4).

JNK activation as measured by the level of phosphorylation of c-Jun on Ser[63] was observed in three of five tumors in MSeC-exposed rats and four of seven tumors from SEL-treated rats (Fig. 4). The level of JNK activation was at least one order of magnitude lower than that observed in ovariectomy rats. The level of the cell survival protein Bcl-2 was not decreased in tumors from Se-treated rats or ovariectomy (Fig. 4), indicating no disabling of Bcl-2 function in mammary tumors containing cells actively engaged in apoptosis induced by Se treatments or ovariectomy.

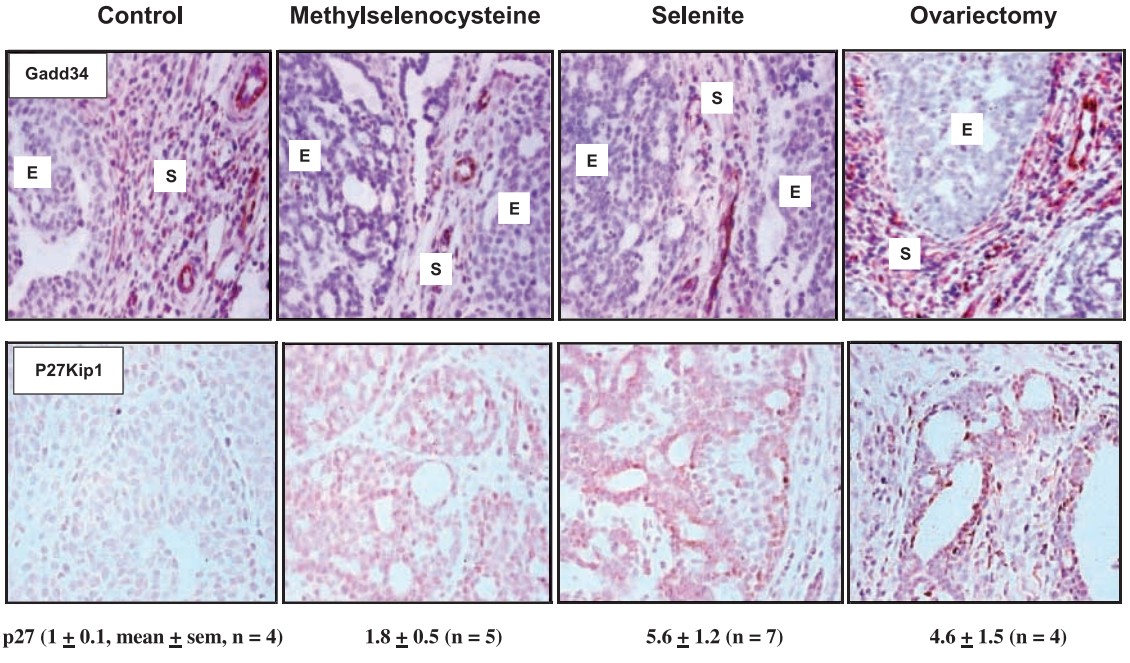

Figure 3. Immunohistochemical detection of gadd34 and P27 proteins in mammary carcinomas after acute treatments with Se compounds or ovariectomy. The gadd34 staining (*top*) was localized in the stromal cell components (*S*) of the mammary carcinoma, most notably in endothelial cells lining microvessels, and absent in the epithelial cells (*E*) before and after Se treatment. P27kip1 staining (*bottom*) was weak in untreated carcinomas. The P27 staining in SEL-, MSeC-, or ovariectomy-treated carcinomas increased over the gavage control carcinomas and was predominantly in the cancerous epithelial cells. The relative P27 staining intensity (by CAS image analyses) in the cancerous epithelial cells compared with the control group was below respective groups.

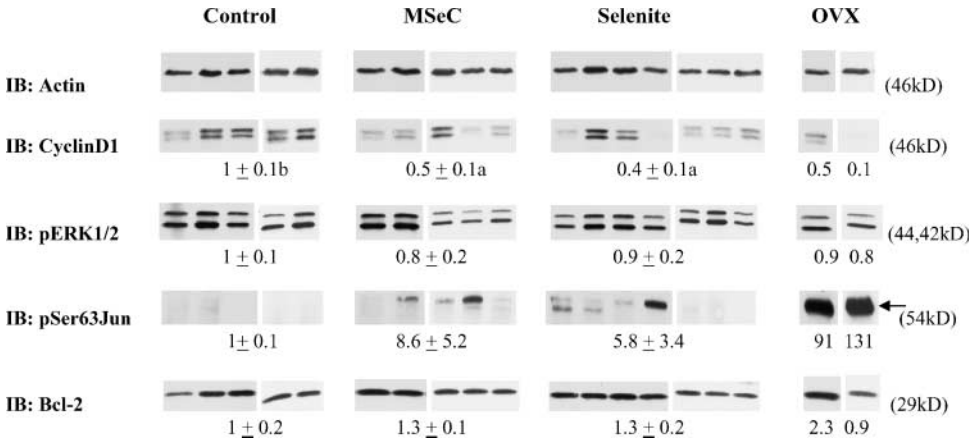

Figure 4. Western blot analyses of growth- and apoptosis-regulatory proteins in mammary carcinomas after acute treatments with Se compounds or ovariectomy. Forty micrograms (by Bradford dye assay) of tumor protein extract were loaded from each sample. β-Actin expression was probed as internal control for loading differences. The normalized pixel densities (expression level) were mean ± SE. Means among groups within a same row with different superscripts were significantly different ($P < 0.05$). Due to the limitation of number of wells on each gel, the carcinomas from each group were analyzed in two different sets and images were compiled later.

Human Prostate Cancer Xenograft Model

To determine whether the lack of *in vivo* induction of *gadd* genes by acute Se treatment was specific to the mammary tumors, we tested the *gadd* expression changes in DU145 prostate cancer cells *in vitro* (Fig. 5A) and in xenograft after treatment with MSeA or MSeC (Fig. 5B and C). We confirmed that in cell culture with DU145 and LNCaP prostate cancer cells, exposure to an apoptotic dose of MSeA for 6 hours strongly activated gadd153 expression (Fig. 5A), as has been reported in PC-3 cells (7, 17). We have previously shown that MSeA and MSeC, given to nude mice at a dose of 4 mg per kilogram of body weight starting 1 day after DU145 cell inoculation, resulted in >50% inhibition of tumor growth in 5 weeks with little adverse effect on body weight (28). Then, we analyzed these xenograft tumors for either the human (Fig. 5B) or murine (Fig. 5C) mRNA for gadd34, gadd45, and gadd153 by real-time RT-PCR and did not detect any increase due to the Se treatments.

To characterize the kinetics of apoptosis in the human xenograft tumors, we carried out an acute treatment experiment in tumor-bearing nude mice after the xenografts had grown to an average size of 150 mm^3 with MSeA (4 mg Se/kg, oral single dose, daily). Tumors were frozen at −70°C until analyzed. Tumors from five mice of each group were pooled (approximately equal weight) for the preparation of tissue lysate for Western blot analysis of biomarkers related to caspase-mediated apoptosis and gadd protein expression.

Increased cleavage of poly(ADP)ribose polymerase was detected at both 24 and 72 hours of MSeA exposure (Fig. 6A). Concomitantly, we detected an activation of caspase-3 cleavage as early as 24 hours and sustained through 72 hours (Fig. 6A). Procaspase-8 cleavage displayed a similar pattern as did caspase-3 (not shown). TUNEL assay for apoptotic fragmented DNA ends detected increased positive signals (Fig. 6B). These data were consistent with increased caspase-mediated apoptosis in human xenograft tumors by MSeA acute exposure.

Western blot analyses did not detect any increased gadd34 abundance or gadd153 (Fig. 6A). A modest decrease of cyclin D1 abundance at both 24 and 72 hours of MSeA treatment was observed whereas a modest induction of P27Kip1 was detected by 72 hours (Fig. 6A).

Discussion

The present work used two acute exposure models to investigate apoptosis induction by Se compounds and the potential *in vivo* molecular targets/biomarkers of the chemotherapeutic action. In the MNU-induced rat mammary carcinogenesis model, we observed that a daily single gavage of either SEL or MSeC (2 mg Se per kilogram of body weight) for 3 days in tumor-bearing female rats led to the regression of a vast majority of the established mammary tumors (Fig. 1C). The observed tumor volume reduction was associated with significantly increased incidence of cancer epithelial apoptosis (Fig. 1D) and moderately decreased rate of BrdUrd incorporation in the cancer cells (Fig. 1E). The dose of SEL or MSeC used here approximated 5- to 10-fold of typical chemopreventive intake (8, 33). Because Ip and coworkers have shown that established tumors in the mammary model did not respond to the typical chemopreventive Se intake (1), we chose the higher dose of Se intending to elicit a measurable tumor volume response in an acute therapy context to enable us to examine whether the *gadd* gene expression changes could be observed *in vivo* and associated with the *in vivo* apoptosis in the cancerous mammary epithelium. The high dose was not acutely lethal to the rats, but nevertheless toxic to them, resulting in a loss of body weight in comparison with gavage control rats (Fig. 1A). However, the tumor-regressing action of Se exposure could not be accounted for by weight loss per se as evident by the lack of any effect of diet restriction that led to a comparable degree of body weight loss on tumor volume. Diet restriction did not inhibit epithelial cell proliferation nor did it induce apoptosis or gene/protein expression changes (Fig. 2).

In an effort to identify potential biomarkers or targets of the proapoptotic and antiproliferative activities of Se *in vivo* observed in this tumor model, we compared the expression patterns of *gadd* gene products and selected cell

cycle and apoptosis regulatory proteins (Figs. 2–4) in the tumors from gavage control and Se-treated tumor-bearing rats. In contrast to the induction effects of Se compounds on *gadd* gene expression in mouse mammary tumor cells observed in cell culture models (5, 9), the steady-state level of mRNA for all three *gadd* genes examined was not higher in Se-treated tumors than in those from the gavage or diet restriction control animals (Fig. 2). Furthermore, the gadd34 and gadd153 protein products were localized in the nonepithelial cells and no induction by Se treatment was detected in the epithelial cells (Fig. 3). These data were inconsistent with a direct mediator role of the *gadd* gene products for the *in vivo* antiproliferative and proapoptotic activity of Se in the mammary tumor epithelial cells, although we could not rule out the possibility that our single time point for harvesting the mammary tumors for analyses might have missed the window of induction of these genes.

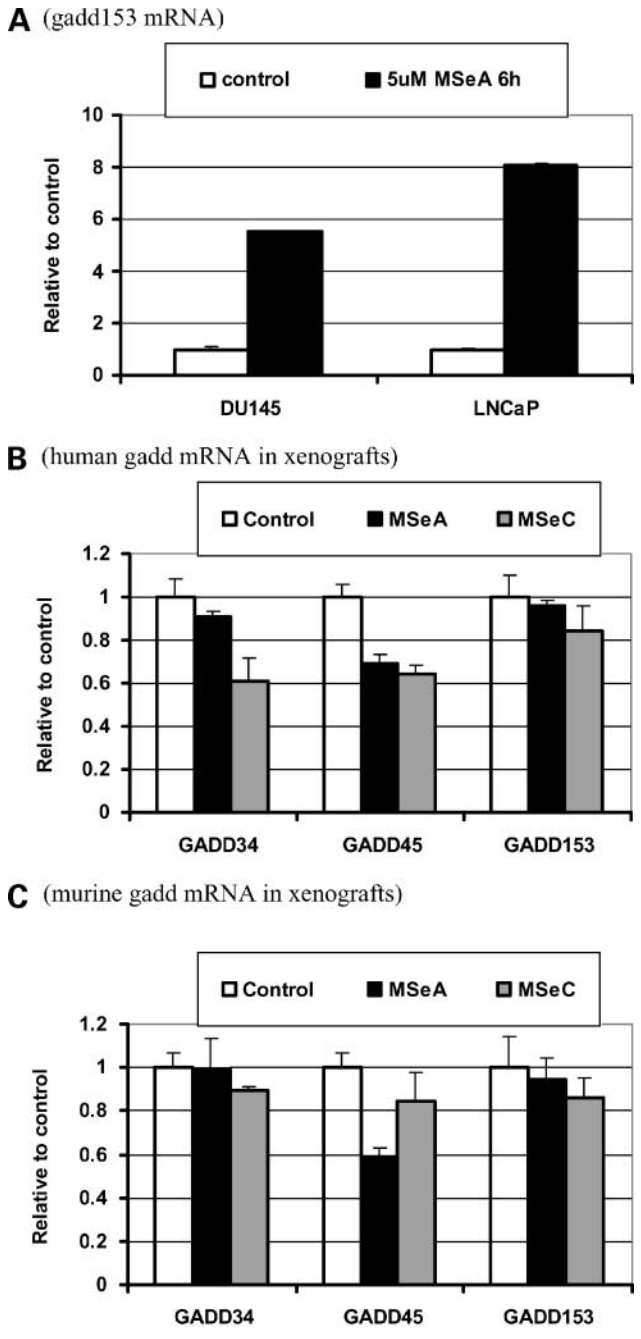

Figure 5. Real-time RT-PCR detection of gadd mRNA in DU145 prostate cancer cells in cell culture or xenograft from nude mice. **A,** induction of gadd153 mRNA level by MSeA after 6-h treatment of DU145 cells. **B,** mRNA level of human gadd34, gadd45, and gadd153 in DU145 xenografts after the tumor-bearing mice has been treated with daily oral gavage 4 mg/kg of MSeA or MSeC for 5 wk (see ref. 28). **C,** mRNA level of murine gadd34, gadd45, and gadd153 in DU145 xenografts from **B**.

To further address this issue and to determine whether the findings were specific to mammary tumors, we examined human prostate cancer xenograft models in nude mice (Fig. 5). The additional work was significant because the prostate has been found to be the most responsive organ site for selenized-yeast intervention of cancer risk in a clinical trial led by the late Dr. Larry Clark (34). Prompted by these encouraging results, the Selenium and Vitamin E Cancer Prevention Trial (SELECT) study (35) was testing the prostate cancer–preventive efficacy of selenomethionine, which is the major Se species present in selenized yeast, and/or vitamin E supplementation in North American men.[4] The enrollment of some 35,500 subjects was completed in June 2004. The selenomethionine intervention was designed for an average of 7 years. The National Cancer Institute stopped the trial in late October 2008, several years ahead of the scheduled completion date, due to a possible increase of diabetes risk in selenomethionine-supplemented subjects and an increase in prostate cancer risk by the vitamin E–supplemented subjects. In hindsight, preclinical prostate cancer models conducted before (36) and since SELECT was initiated (28, 37) did not support any *in vivo* anticancer activity of selenomethionine. Whereas the SELECT results convincingly ruled out selenomethionine for prostate cancer prevention, *in vivo* preclinical mechanistic studies of other Se forms will help to critically judge their potential utility as candidate compounds in future clinical trials. Much work since the original Clark study has focused on prostate cancer cell lines with Se forms much more active than selenomethionine, identifying numerous signaling pathways (8), including *gadd* genes (7, 17, 18). However, none of the studies dealt with *in vivo* validation of the molecular targets or cellular pathways.

Same as in the mammary tumors, we did not detect increased mRNA level for the three *gadd* genes in the human DU145 prostate cancer xenograft after MSeA or MSeC treatment (Fig. 5B and C), in spite of significant induction in cell culture by MSeA as shown in Fig. 5A or as reported in PC-3 cells (7, 17, 18). In the acute exposure context, we failed to detect increased gadd34 or gadd153 protein (Fig. 6A)

[4] http://www.cancer.gov/clinicaltrials/digestpage/SELECT

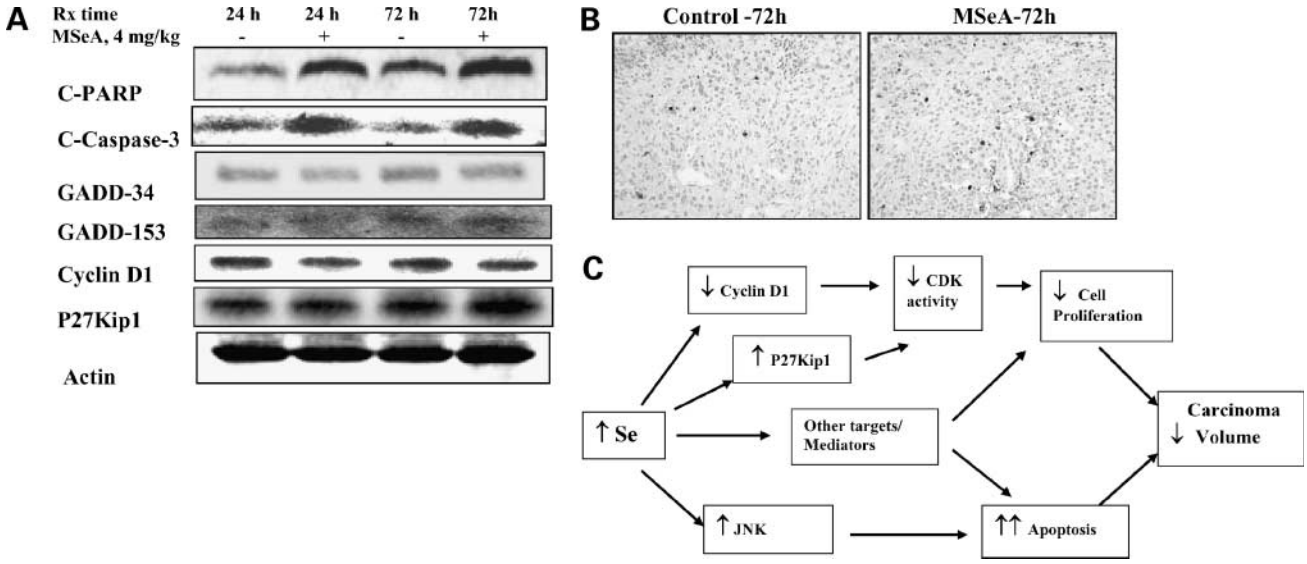

Figure 6. Apoptosis response of human DU145 prostate cancer xenograft in nude mice after acute exposure to MSeA. **A,** Western blot analyses of growth and apoptosis regulatory proteins in DU145 prostate cancer xenograft after acute treatments of tumor-bearing mice with MSeA (4 mg/kg) for 24 or 72 h. Protein extract was prepared from pooled sample of five to six tumors. β-Actin expression was probed as internal control for loading differences. **B,** TUNEL detection of increased apoptosis (*dark stains*) after 72-h treatment with MSeA. **C,** schematic pathway links of *in vivo* Se treatment to apoptosis and growth inhibition in cancer cells.

although we detected increased caspase-mediated apoptosis (Fig. 6A and B). Taken together, both the mammary and prostate models failed to link the *in vivo* apoptosis and antiproliferation actions of Se to these *gadd* genes.

The disconnect between *in vitro* induction of *gadd* genes by Se and the lack of involvement in the two *in vivo* cancer models is not surprising. Cell culture models measure, by and large, the direct effects of Se compounds on target cancer cells but rarely simulate *in vivo* hepatic and systemic Se metabolism. *In vivo* metabolism could have resulted in Se forms that came in contact with the cancer cells very different from what were given to the animals. Our current work highlights the risk of missing the mark when cell culture models are used as target discovery tools for compounds that may undergo extensive *in vivo* metabolism.

On the other hand, our results suggested the potential involvement of cyclin D1, P27Kip1, and the JNK pathway in growth arrest and apoptosis induced by Se exposure *in vivo*. Cyclin D1 expression, at both mRNA and protein levels, was decreased in most of the Se-treated tumors (Figs. 2 and 4) and in prostate xenograft (Fig. 6). P27Kip1 expression was induced in the tumor epithelial cells by SEL and to a lesser extent by MSeC exposure (Fig. 3). Consistent with this acute exposure model, chronic feeding of MSeC to MNU-treated rats led to the increased expression of P27 in intraductal proliferation lesions, which represent an early stage of mammary carcinogenesis progression (38). Because cyclin D1 and P27 are respective positive and negative regulators of CDK activities, the observed induction of P27 and reduction of cyclin D1 expression by acute Se exposure suggest a potential *in vivo* mechanism for Se to arrest cell cycle progression through modulating the activities of CDK4, leading to growth arrest (Fig. 6C). In addition, the observed *in vivo* proapoptotic effect of Se may be facilitated by perturbed survival/apoptosis signals through stress-activated protein kinase pathways. The observed JNK activation in some Se-treated mammary carcinomas (Fig. 4) lends credence to this postulate (Fig. 6C).

In summary, the lack of up-regulation by Se treatments on the *in vivo* expression of *gadd* genes in two preclinical animal cancer models cast doubt on their role as potential mediators of the antiproliferative and proapoptotic activity of Se. The observed reduction of cyclin D1 expression, induction of P27Kip1, and the activation of JNK in a majority of the Se-exposed mammary carcinomas implicated their potential involvement in the Se actions *in vivo*.

Disclosure of Potential Conflicts of Interest

All authors have no personal or financial conflict of interest and have not entered into any agreement that could interfere with our access to the data on the research or on our ability to analyze the data independently, to prepare manuscripts, and to publish them.

Acknowledgments

We thank Dr. Howard Ganther, University of Wisconsin, Madison, for generously providing the Se-methylselenocysteine used in the mammary cancer study; the following former colleagues at AMC Cancer Research Center for valuable contribution to the execution of this project: Dr. Henry Thompson for guidance on the chemical mammary carcinogenesis model, Kim Rothhammer for excellent animal care and animal surgery, Dr. Zaisen Wang and Nathan Glasgow for performing Se analysis, John McGinley for expert advice on immunohistochemistry, and Dr. Zongjian Zhu for statistical evaluations; and Dr. Guang-xun Li for the prostate xenograft tissues.

References

1. Ip C, Lisk DJ, Thompson HJ. Selenium-enriched garlic inhibits the early stage but not the late stage of mammary carcinogenesis. Carcinogenesis 1996;17:1979 – 82.

2. Lu J, Pei H, Ip C, Lisk DJ, Ganther H, Thompson HJ. Effect of an aqueous extract of selenium-enriched garlic on *in vitro* markers and *in vivo* efficacy in cancer prevention. Carcinogenesis 1996;17:1903 – 7.

3. Lu J, Jiang C, Kaeck M, et al. Dissociation of the genotoxic and growth inhibitory effects of selenium. Biochem Pharmacol 1995;50:213 – 9.

4. Lu J, Kaeck M, Jiang C, Wilson AC, Thompson HJ. Selenite induction of DNA strand breaks and apoptosis in mouse leukemic L1210 cells. Biochem Pharmacol 1994;47:1531 – 5.

5. Kaeck M, Lu J, Strange R, Ip C, Ganther HE, Thompson HJ. Differential induction of growth arrest inducible genes by selenium compounds. Biochem Pharmacol 1997;53:921 – 6.

6. Jiang C, Wang Z, Ganther H, Lu J. Caspases as key executors of methyl selenium-induced apoptosis (anoikis) of DU-145 prostate cancer cells. Cancer Res 2001;61:3062 – 70.

7. Wu Y, Zhang H, Dong Y, Park YM, Ip C. Endoplasmic reticulum stress signal mediators are targets of selenium action. Cancer Res 2005;65: 9073 – 9.

8. Lu J, Jiang C. Selenium and cancer chemoprevention: hypotheses integrating the actions of selenoproteins and selenium metabolites in epithelial and non-epithelial target cells. Antioxid Redox Signal 2005;7: 1715 – 27.

9. Sinha R, Kiley SC, Lu JX, et al. Effects of methylselenocysteine on PKC activity, cdk2 phosphorylation, and gadd gene expression in synchronized mouse mammary epithelial tumor cells. Cancer Lett 1999;146:135 – 45.

10. Fornace AJ, Jr., Alamo I, Jr., Hollander MC. DNA damage-inducible transcripts in mammalian cells. Proc Natl Acad Sci U S A 1988;85:8800 – 4.

11. Fornace AJ, Jr., Nebert DW, Hollander MC, et al. Mammalian genes coordinately regulated by growth arrest signals and DNA-damaging agents. Mol Cell Biol 1989;9:4196 – 203.

12. Luethy JD, Holbrook NJ. Activation of the gadd153 promoter by genotoxic agents: a rapid and specific response to DNA damage. Cancer Res 1992;52:5 – 10.

13. Ron D, Habener JF. CHOP, a novel developmentally regulated nuclear protein that dimerizes with transcription factors C/EBP and LAP and functions as a dominant-negative inhibitor of gene transcription. Genes Dev 1992;6:439 – 53.

14. Zhan Q, Lord KA, Alamo I, Jr., et al. The gadd and MyD genes define a novel set of mammalian genes encoding acidic proteins that synergistically suppress cell growth. Mol Cell Biol 1994;14:2361 – 71.

15. Zhan Q, Bae I, Kastan MB, Fornace AJ, Jr. The p53-dependent γ-ray response of GADD45. Cancer Res 1994;54:2755 – 60.

16. Oyadomari S, Mori M. Roles of CHOP/GADD153 in endoplasmic reticulum stress. Cell Death Differ 2004;11:381 – 9.

17. Dong Y, Zhang H, Hawthorn L, Ganther HE, Ip C. Delineation of the molecular basis for selenium-induced growth arrest in human prostate cancer cells by oligonucleotide array. Cancer Res 2003;63:52 – 9.

18. Zu K, Bihani T, Lin A, Park YM, Mori K, Ip C. Enhanced selenium effect on growth arrest by BiP/GRP78 knockdown in p53-null human prostate cancer cells. Oncogene 2006;25:546 – 54.

19. Davis RJ. Signal transduction by the JNK group of MAP kinases. Cell 2000;103:239 – 52.

20. Xia Z, Dickens M, Raingeaud J, Davis RJ, Greenberg ME. Opposing effects of ERK and JNK-p38 MAP kinases on apoptosis. Science 1995; 270:1326 – 31.

21. Dent P, Yacoub A, Fisher PB, Hagan MP, Grant S. MAPK pathways in radiation responses. Oncogene 2003;22:5885 – 96.

22. Sherr CJ, Roberts JM. CDK inhibitors: positive and negative regulators of G_1-phase progression. Genes Dev 1999;13:1501 – 12.

23. Sherr CJ, Roberts JM. Living with or without cyclins and cyclin-dependent kinases. Genes Dev 2004;18:2699 – 711.

24. Sicinski P, Donaher JL, Parker SB, et al. Cyclin D1 provides a link between development and oncogenesis in the retina and breast. Cell 1995;82:621 – 30.

25. Thompson HJ, McGinley JN, Rothhammer K, Singh M. Rapid induction of mammary intraductal proliferations, ductal carcinoma *in situ* and carcinomas by the injection of sexually immature female rats with 1-methyl-1-nitrosourea. Carcinogenesis 1995;16:2407 – 11.

26. Thompson HJ, McGinley J, Rothhammer K, Singh M. Ovarian hormone dependence of premalignant and malignant mammary gland lesions induced in pre-pubertal rats by 1-methyl-1-nitrosourea. Carcinogenesis 1998;19:383 – 6.

27. McGinley JN, Knott KK, Thompson HJ. Effect of fixation and epitope retrieval on BrdU indices in mammary carcinomas. J Histochem Cytochem 2000;48:355 – 62.

28. Li GX, Lee HJ, Wang Z, et al. Superior *in vivo* inhibitory efficacy of methylseleninic acid against human prostate cancer over selenomethionine or selenite. Carcinogenesis 2008;29:1005 – 12.

29. Bodis S, Siziopikou KP, Schnitt SJ, Harris JR, Fisher DE. Extensive apoptosis in ductal carcinoma *in situ* of the breast. Cancer 1996;77: 1831 – 5.

30. McGinley JN, Knott KK, Thompson HJ. Semi-automated method of quantifying vasculature of 1-methyl-1-nitrosourea-induced rat mammary carcinomas using immunohistochemical detection. J Histochem Cytochem 2002;50:213 – 22.

31. Jiang C, Jiang W, Ip C, Ganther H, Lu J. Selenium-induced inhibition of angiogenesis in mammary cancer at chemopreventive levels of intake. Mol Carcinog 1999;26:213 – 25.

32. Thompson HJ, Zhu Z, Jiang W. Identification of the apoptosis activation cascade induced in mammary carcinomas by energy restriction. Cancer Res 2004;64:1541 – 5.

33. Ip C. Lessons from basic research in selenium and cancer prevention. J Nutr 1998;128:1845 – 54.

34. Clark LC, Combs GF, Jr., Turnbull BW, et al. Effects of selenium supplementation for cancer prevention in patients with carcinoma of the skin. A randomized controlled trial. Nutritional Prevention of Cancer Study Group. JAMA 1996;276:1957 – 63.

35. Lippman SM, Goodman PJ, Klein EA, et al. Designing the Selenium and Vitamin E Cancer Prevention Trial (SELECT). J Natl Cancer Inst 2005; 97:94 – 102.

36. McCormick DL, Rao KV. Chemoprevention of hormone-dependent prostate cancer in the Wistar-Unilever rat. Eur Urol 1999;35:464 – 7.

37. Corcoran NM, Najdovska M, Costello AJ. Inorganic selenium retards progression of experimental hormone refractory prostate cancer. J Urol 2004;171:907 – 10.

38. Ip C, Thompson HJ, Ganther HE. Selenium modulation of cell proliferation and cell cycle biomarkers in normal and premalignant cells of the rat mammary gland. Cancer Epidemiol Biomarkers Prev 2000;9:49 – 54.